Novak (Cornell U. P., Ithaca, NY, 1987), p. 84.
[7]F. Reif, "Teaching problem solving—A scientific approach," Phys. Teach. **19**, 310–316 (1981).
[8]R. G. Van Ausdal, "Structural problem solving in kinematics," Phys. Teach. **26**, 518–522 (1988).
[9]D. P. Maloney, "Forces as interactions," Phys. Teach. **28**, 386–390 (1990).
[10]D. P. Maloney, "Fill-in problems," J. Coll. Sci. Teach. **12**, 104–106 (1982).
[11]I. A. Halloun and D. Hestenes, "Common sense concepts about motion," Am. J. Phys. **53**, 1056–1065 (1985).
[12]Personal communication from Randy Knight.

Dynamical symmetry breaking and chaos in Duffing's equation

Collin L. Olson and M. G. Olsson
Department of Physics, University of Wisconsin, Madison, Wisconsin 53706

(Received 4 October 1990; accepted for publication 7 March 1991)

In certain frequency ranges a nonlinear damped and driven oscillator will respond asymmetrically even though the potential energy is a single symmetric well. This dynamical symmetry breaking heralds the onset of a period doubling transition to chaos.

A driven damped oscillator with a nonlinear spring can be thought of as the "hydrogen atom" of chaos. A mass m subject to a spring force

$$F(x) = -m(\omega_0^2 x + \beta x^3), \tag{1}$$

with linear damping $F = -2m\gamma\dot{x}$ and a sinusoidal driving force $F = mf\cos\omega t$, satisfies Duffing's equation[1]

$$\ddot{x} + 2\gamma\dot{x} + \omega_0^2 x + \beta x^3 = f\cos\omega t. \tag{2}$$

Many of the properties of this equation are well known both in monographs[2] and in this journal.[3] The perturbative solutions, jumps, hysteresis, and harmonic resonances form an almost classical body of knowledge. The transition to chaos also has been carefully investigated but primarily for the double-well case[4] resulting, for example, when $\omega_0^2 = -1$ and $\beta = +1$.

Our purpose here is to emphasize and enlarge upon a deceptively simple example: that of a single symmetric potential well resulting when both ω_0^2 and β are positive. The attraction of this case lies in the simplicity of the potential energy, as shown in Fig. 1. It is straightforward to demonstrate that if ω_0^2 and β are positive, a rescaling of coordinate and time reduces Duffing's equation (2) to a normal form:

$$\ddot{x} + 2\gamma\dot{x} + x + x^3 = f\cos\omega t. \tag{3}$$

In this form the underlying parameters of the system are the damping constant γ, the driving amplitude f, and the driving frequency ω. We shall fix the damping at

$$\gamma = \tfrac{1}{10}, \tag{4}$$

and vary the driving parameters f and ω.

For $f \ll 1$ the excitation is nearly linear and the anharmonic effects are easily calculated using perturbation theory. By $f = \frac{1}{2}$ the hysteresis effect at the primary resonance is quite evident and harmonic resonances with peaks at $\omega_{\text{res}} \simeq (2n+1)^{-1}$ are starting to appear. After many cycles of the oscillator, the transients die out and the *attractor* remains. If the response has the same period as the driver, we have a *periodic attractor*. In Fig. 2 we show the maximum displacement (or amplitude) of the attractor for $f = 3$ for a range of frequencies sweeping both up and down.[5] The hysteresis in the primary resonance is clearly marked, and a lowest-order perturbation curve is included to show the jumps from one stable branch to the other during the frequency sweep. The harmonic resonance peaks are labeled by their Fourier components.

The *Poincaré section* is particularly useful in identifying the onset of chaotic motion. In this picture we concentrate

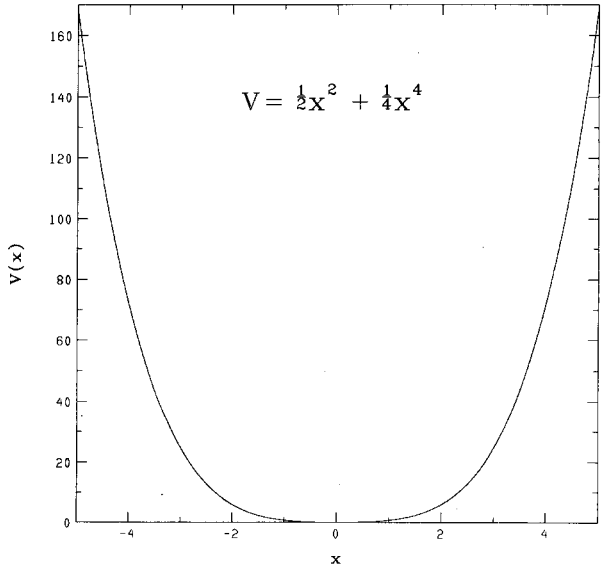

Fig. 1. Hard-spring potential energy (with $m = \omega_0^2 = \beta = 1$) corresponding to the nonlinear spring force of Eq. (1).

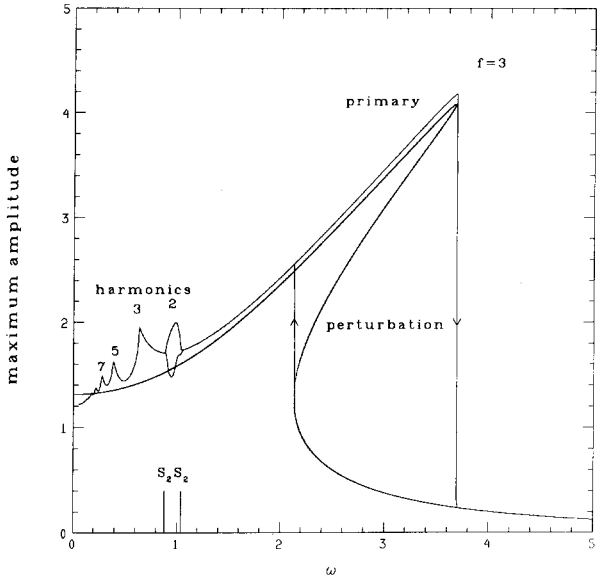

Fig. 2. Maximum displacement of Duffing's oscillator with $f = 3$. The driving frequency was varied both up and down in small increments. Mechanical hysteresis is observed with sudden jumps between the two stable attractors. The lowest-order perturbative result is shown for comparison. Harmonic resonances are labeled by their Fourier component, and the dynamical symmetry-breaking region S_2S_2' is indicated.

on the oscillator response at a particular phase of the driving force. If the asymptotic orbit is reentrant after one period of the driver, the mass is always in the same state each period. The Poincaré section of this periodic attractor will give a single point in the $(x,\dot{x})$ plane. For frequencies below the primary resonance, the response $x(t)$ is roughly in phase with the driver, while the response is opposite the driver at high frequencies. The Poincaré section is thus quite similar to the maximum amplitude plot away from resonances. Figure 3 illustrates the frequency dependence of the x component of the Poincaré section when $f = 3$. This figure should be compared carefully to the maximum amplitude plot of Fig. 2.

In Figs. 2 and 3 there is a region[6] (denoted by S_2S_2') where an even-harmonic amplitude is present. A Fourier analysis for $f = 3$ shows directly that in the frequency region $0.88 < \omega < 1.05$ the second harmonic (with frequency 2ω) begins and ends. The solution otherwise contains only odd harmonics. Because the potential energy is symmetric about $x = 0$, we might have anticipated that the response would also be symmetric. The actual behavior in this angular frequency range is an example of *dynamical symmetry breaking*. The response is not symmetric even though the spring potential is.

As shown in Ref. 6, other symmetry-breaking regimes appear between the odd-harmonic resonance at higher driving amplitudes f. In both Figs. 2 and 3 there seem to be two stable amplitudes in the S_2S_2' region. This is only apparent since there are two otherwise identical ways to break the symmetry corresponding to a larger right-turning point or a larger left-turning point. The second solution is just the back side of the alternative symmetry-breaking orbit.

We shall emphasize in this article how the S_2S_2' region evolves as the driving amplitude f is increased. From $f = 3$ to 15 the symmetry-breaking region will exhibit increasing hysteresis and more exaggerated frequency dependence of the orbit. At $f = 20$ we observe clearly the first true period-doubling bifurcation, and at $f = 25$ there is a full cascade of bifurcations leading to chaotic behavior.

A magnified Poincaré view of the S_2S_2' frequency region when $f = 5$ is given in Fig. 4. Within the S_2S_2' region two curves are shown, indicating that the attractor is asymmetric. For driving frequencies above and below this region, the solution is symmetric, but between S_2 and S_2' the dynamical symmetry breaking due to the double-frequency amplitude causes the turning points to be different distances from the origin. Even though the Poincaré section is

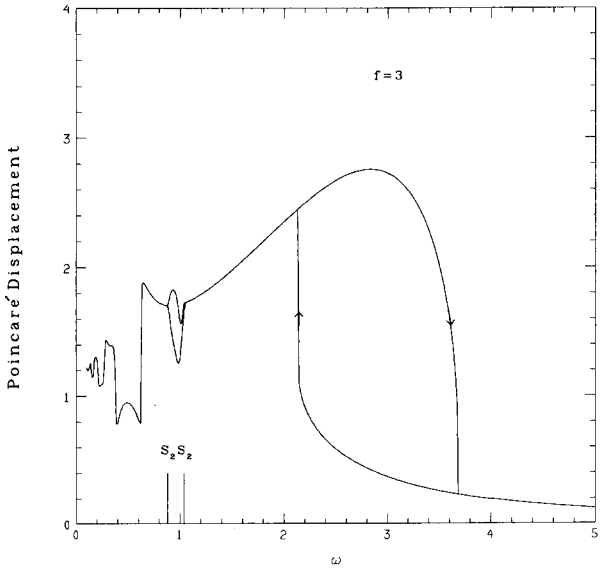

Fig. 3. Displacement component of the Poincaré section at zero driver phase and $f = 3$ driving amplitude. All subsequent Poincaré plots are also at zero driving phase.

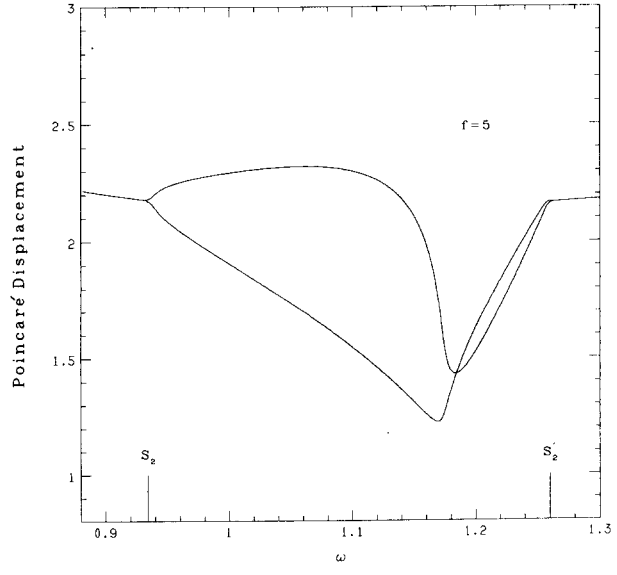

Fig. 4. $f = 5$ Poincaré displacement in the S_2S_2' region. The two attractors are the two symmetry-breaking cases. They correspond to the same orbit.

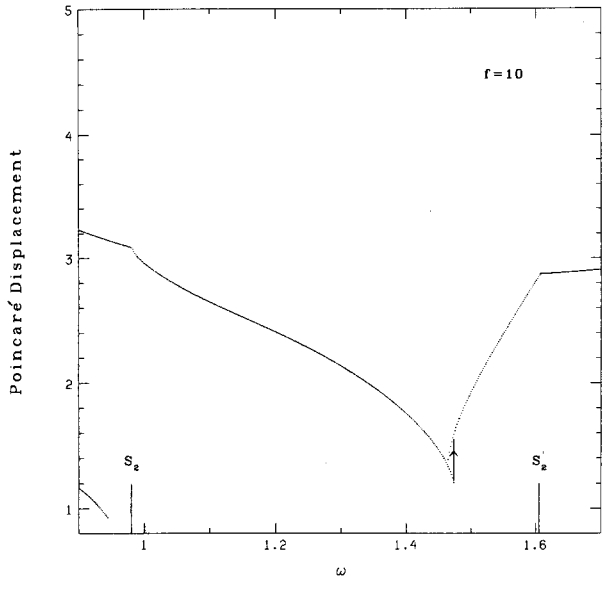

Fig. 5. $f = 10$ Poincaré displacement. Only one symmetry-breaking attractor is shown. Mechanical hysteresis begins to appear near $\omega = 1.47$.

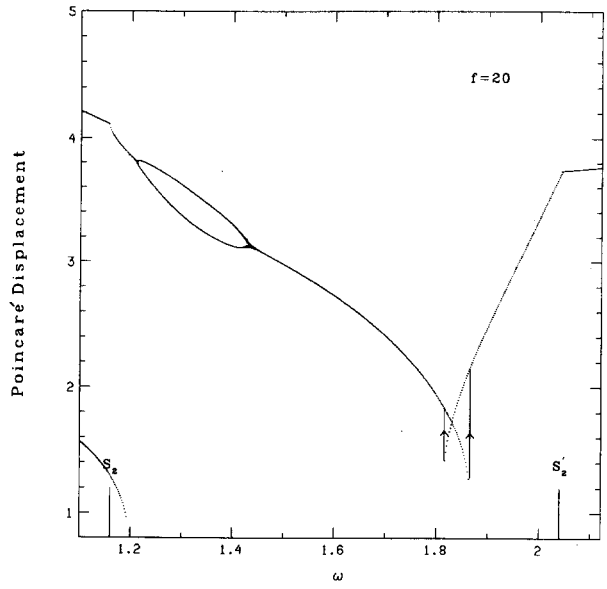

Fig. 7. $f = 20$ Poincaré displacement. A period-doubling bifurcation appears between $1.2 < \omega < 1.4$. The hysteresis near $\omega = 1.8$ has become prominent. Again, only one symmetry-breaking attractor is shown. The other branch, as in Fig. 4, is the other side of the same orbit.

taken at zero phases of the driver, there are two equivalent orbits corresponding to the two ways that the symmetry can be broken. Another interesting process which goes on in this region is a change in the number of orbit loops in the $(x,\dot{x})$ plane. Both above S_2' and below S_2, the orbit is a simple curve with only one maximum and one minimum displacement. As one raises the driving frequency above S_2, a loop will form, and for a part of the interval between S_2 and S_2' there will be four turning points ($\dot{x} = 0$).

Figures 5 and 6 depict the Poincaré displacements when $f = 10$ and 15. Very little qualitatively changes at these larger driving amplitudes other than the development of some hysteresis at the minimum Poincaré displacement. Only one of the two possible Poincaré displacements is shown. We sweep up and down in frequency to show the hysteresis.

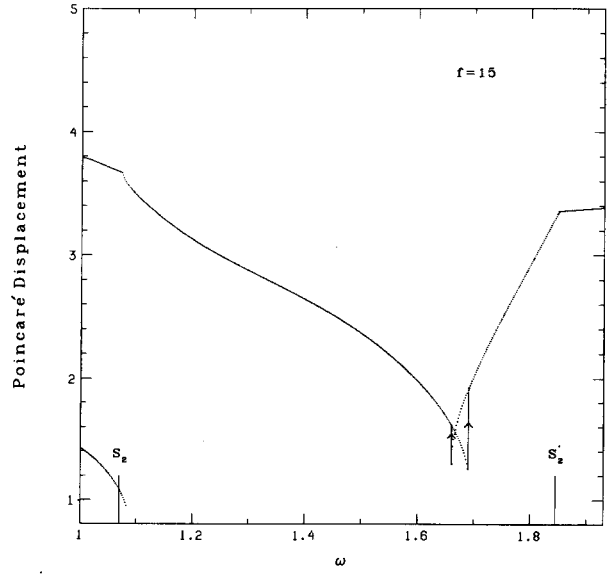

Fig. 6. $f = 15$ Poincaré displacement.

When the driving amplitude is increased to $f = 20$, the first true period-doubling bifurcation now becomes clearly evident. The fact that it is preceded by a symmetry-breaking bifurcation is general in symmetric systems.[7] The Poincaré displacement at $f = 20$ is shown in Fig. 7. The phase-space $(x,\dot{x})$ orbits at $\omega = 1.4$ and 1.45 are illustrated in Fig. 8. Comparison of these two figures shows that in the bifurcation region two orbits are required for periodicity. If the Fourier spectrum were computed in the frequency range of Fig. 7, a $\frac{1}{2}\omega t$ component would appear in the bifurcation region and nowhere else. This is consistent with the observed period doubling.

A further increase in the driving amplitude to $f = 25$ produces a complete cascade of bifurcations and a chaotic region as shown in Fig. 9. Again, we have suppressed the branch corresponding to the alternate symmetry breaking except in the region near $\omega \simeq 1.3$, where the chaotic regions of the two branches overlap. Figure 10 shows a more detailed view of the initial part of the bifurcation region, revealing a complete cascade of period doublings. The similarity to the well-known logistic or quadratic iterative map is striking.

Slightly beyond the accumulation point of the bifurcation sequence lies a region of chaotic motion. At $\omega = 1.2902$ we show in Fig. 11 the full Poincaré section, again at zero driving phase. This time, instead of a finite number of attractor points, a more elaborate attractor is traced out. Figure 11 exhibits the result of 10 000 oscillator cycles or 10 000 Poincaré points. An attractor of this sort is known as a *strange attractor*. It apparently consists of curves in the $(x,\dot{x})$ plane, but upon closer examination these curves are found to have internal structure. A closer view of the portion of the attractor within the rectangle in Fig. 11 is shown in Fig. 12. In principle, this magnification can be continued much as with the Henon map,[8] but numerical limitations soon intercede.

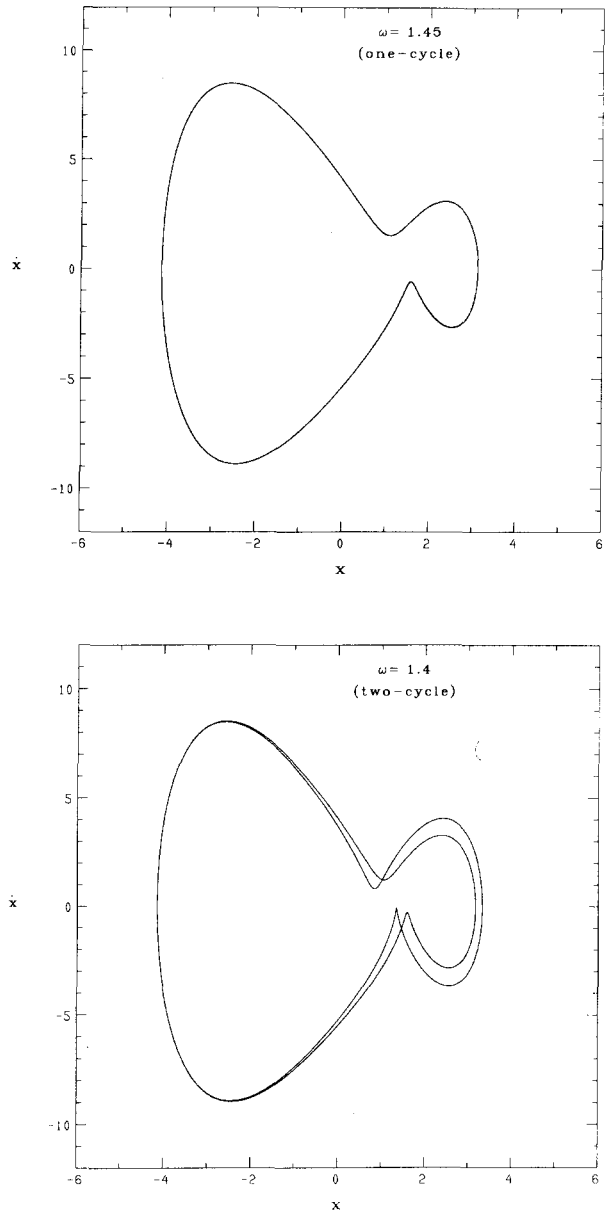

Fig. 8. Orbits in the $(x,\dot{x})$ plane for $f = 20$: (a) $\omega = 1.45$, a periodic attractor; (b) $\omega = 1.40$, a period-doubled (two-cycle) attractor.

The similarity between Duffing's strange attractor and the Henon strange attractor is also compelling. The self-similarity of the Henon attractor with increasing magnification levels is characteristic of a point set of fractal dimension. The fractal (or Hausdorf) dimension of the Henon strange attractor is roughly $\frac{5}{4}$, i.e., between a line and an area. In the Duffing case at $f = 25$, with a further increase in frequency, the attractor collapses back in a reverse-bifurcation sequence and again becomes simple near $\omega = 1.6$.

We have hardly touched upon the complexity of Duffing's oscillator even with monochromatic excitation. Besides regions of symmetry breaking at large amplitudes,[6] these are coexisting attractors, numerous changes in the number of turning points (or winding number), and many harmonic resonances. Although the oscillator response can be quite complex, we believe that this discussion at least

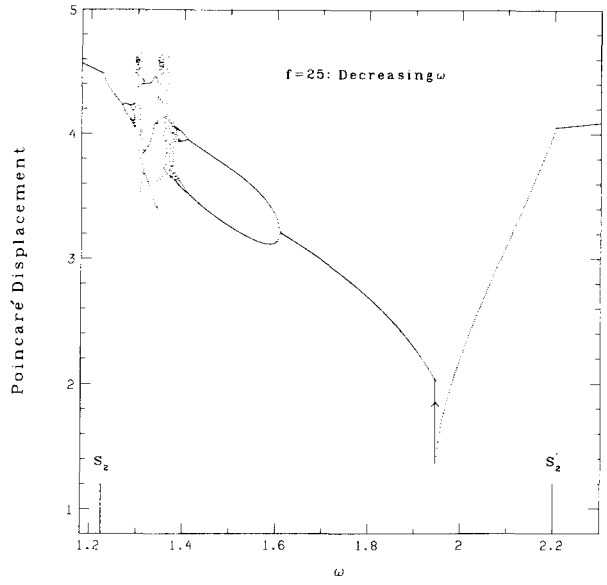

Fig. 9. $f = 25$ Poincaré displacement. The plot is based only on a downward frequency sweep. A complete cascade of period-doubling bifurcations and a reverse sequence occurs. A region of chaos occurs between these cascades. Near $\omega = 1.33$, a three-cycle appears.

gives a feeling for the kind of behavior encountered. We have indicated the relationship between period-doubling-type bifurcations and symmetry-breaking bifurcations which appear similar on the Poincaré plot, but which do not both involve true period doubling. Most previous work on Duffing's equation has focused upon the double-well case where a rich panoply of chaotic motion is also found. The double-well case, however, has built in the added complication of two harmonic basins. Other work on Duffing's equation considers only the cubic force term.[9] We have found it to be quite instructive to explore the hard-spring

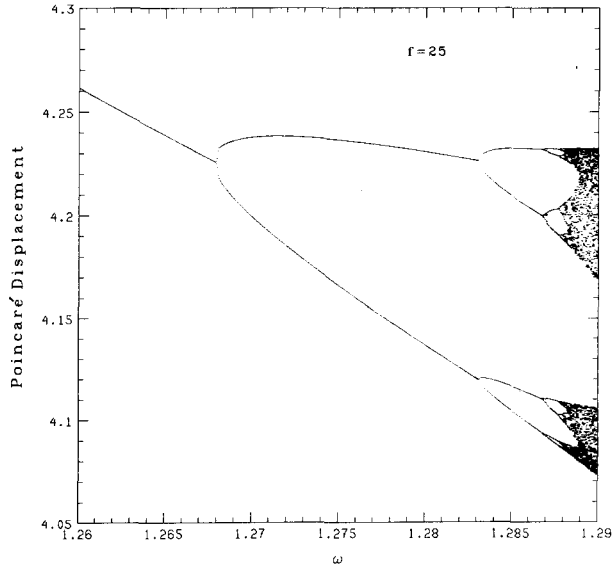

Fig. 10. $f = 25$ Poincaré displacement detail of the bifurcation cascade. The similarity to the logistic map cascade should be noted.

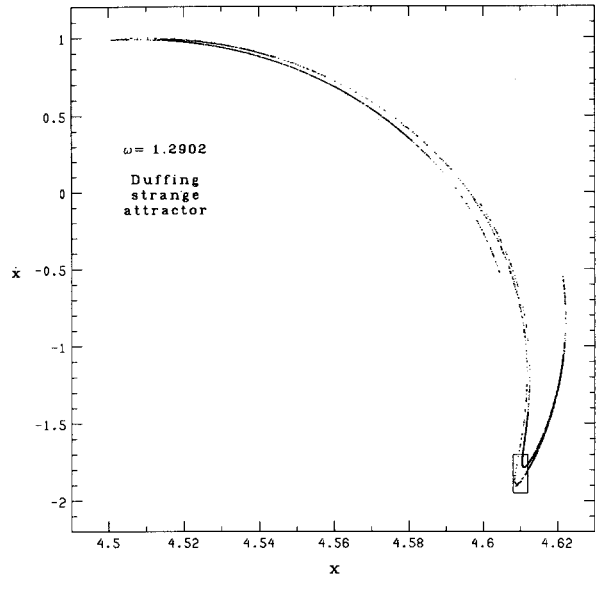

Fig. 11. $f = 25$ Poincaré strange attractor at $\omega = 1.2902$ based on 10 000 cycles.

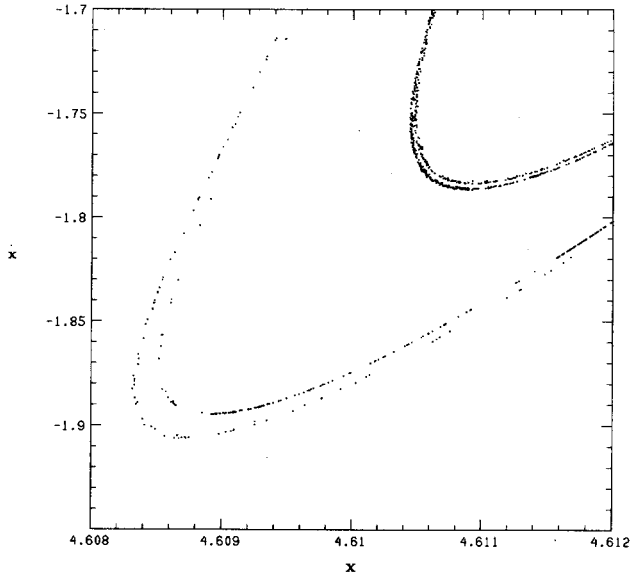

Fig. 12. Blowup of the strange attractor of Fig. 11 contained in the rectangle. This plot was based on 30 000 orbits.

case where perturbative behavior blends into a transition to chaos.

ACKNOWLEDGMENTS

This research was supported in part by the University of Wisconsin Research Committee with funds granted by the Wisconsin Alumni Research Foundation, and in part by the U.S. Department of Energy under Contract DE-AC02-76ER00881.

[1]G. Duffing, *Erzwungene Schwingungen bei Veränderlicher Eigenfrequenz und ihre Technische Bedeutung* (Vieweg, Braunschweig, 1918).

[2]N. Minorsky, *Nonlinear Oscillation* (Krieger, Huntington, N.Y., 1974); J. J. Stoker, *Nonlinear Vibrations* (Interscience, New York, 1950); A. H. Nayfeh and D. T. Mook, *Nonlinear Oscillations, Pure and Applied Mathematics* (Wiley, New York, 1979); F. C. Moon, *Chaotic Vibrations* (Wiley, New York, 1987).

[3]Nicholas B. Tufillaro, "Nonlinear and chaotic string vibrations," Am. J. Phys. **57**, 408–414 (1989).

[4]F. C. Moon and P. J. Holmes, "A magnetoelastic strange attractor," J. Sound Vib. **65**, 275–296 (1979); **69**, 339 (1980); F. C. Moon and G.-X. Li, "Fractal basin boundaries and homoclinic orbits for periodic motion in a two-well potential," Phys. Rev. Lett. **55**, 1439–1442 (1985); P. A. Holmes, "A nonlinear oscillator with a strange attractor," Philos. Trans. R. Soc. London **292**, 420–446 (1979); Sergio De Souza-Machado, R. W. Rollins, D. T. Jacobs, and J. L. Hartman, "Studying chaotic systems using microcomputer simulations and Lyapunov exponents," Am . J. Phys. **58**, 321–329 (1990).

[5]The orbits were calculated using the fourth-order Runge–Kutta method with step sizes between 100 and 2000 steps per driving period, as required for convergence.

[6]Ulrich Parlitz and Werner Lauterborn, "Superstructure in the bifurcation set of the Duffing equation," Phys. Lett. A **107**, 351–355 (1985).

[7]James W. Swift and Kurt Wiesenfeld, "Suppression of period doubling in symmetric systems," Phys. Rev. Lett. **52**, 705–708 (1984).

[8]M. Hénon, "A two-dimensional mapping with a strange attractor," Commun. Math. Phys. **50**, 69–77 (1976); R. L. Devaney, *An Introduction to Chaotic Dynamical Systems* (Addison-Wesley, new York, 1987).

[9]Yashisuke Ueda, "Randomly transitional phenomena in the system governed by Duffing's equation," J. Stat. Phys. **20**, 181–196 (1989); Shinichi Sato, Masaki Sano, and Yasuji Sawada, "Universal scaling property in bifurcation structure of Duffing's and of generalized Duffing's equation," Phys. Rev. A **28**, 1654–1658 (1983).